

# NEW SOPHISTICATED ANALYSIS METHOD OF CRYSTALLIZER TEMPERATURE PROFILE UTILIZING OPTICAL FIBER DTS BASED ON THE STIMULATED RAMAN SCATTERING

Petr KOUDELKA<sup>1</sup>, Andrej LINER<sup>1</sup>, Martin PAPES<sup>1</sup>, Jan LATAL<sup>1</sup>, Vladimír VASINEK<sup>1</sup>, Jan HURTA<sup>2</sup>, Tomas VINKLER<sup>1</sup>, Petr SISKÁ<sup>1</sup>

<sup>1</sup>Department of Telecommunications, Faculty of Electrical Engineering and Computer Science, VSB-Technical University of Ostrava, 17. listopadu 15, 708 33 Ostrava-Poruba, Czech Republic

<sup>2</sup>Laboratory Building Materials, Faculty of Civil Engineering, VSB-Technical University of Ostrava, Ludvika Podestě 1875/17, 708 33 Ostrava-Poruba, Czech Republic

petr.koudelka@vsb.cz, andrej.liner@vsb.cz, martin.papes@vsb.cz, jan.latal@vsb.cz, vladimir.vasinek@vsb.cz, jan.hurta@vsb.cz, tomas.vinkler.st1@vsb.cz

**Abstract.** Continuous casting is a modern and advanced technology of steel production, whose product is a steel blank as a semifinished product for further manufacturing. It is known that better monitoring and process control of casting improves the steel quality and is able to ensure customers' requirements in terms of sizes, brands, quantities and properties with lower costs. The crystallizer belongs among the most important parts of this whole process [1]. At present many methods for analysing of the crystallizer temperature profile in operation were published and experimentally verified. In these methods, the thermocouples or Bragg gratings are widely used. New sophisticated analysis method of crystallizer temperature profile is the utilization of the optical fiber DTS based on the stimulated Raman scattering. This paper describes the first experimental measurement and verification of the method, which are necessary for the method deployment into the industrial practices.

## Keywords

*Casting of steel, crystallizer, fiber optic DTS, fiber optic meander in point mode, stimulated Raman scattering.*

## 1. Crystallizer and its Functions

The main function of the crystallizer is to ensure stiffening of the surface shell of such a thickness and strength that will keep the content of a liquid core inside at the iron stream input into the secondary cooling zone. The key parameters are shape, shell thickness, the same

temperature of the shell during the shift and this all without the internal and surface defects with minimal porosity and a small number of non-metallic inclusions [2].

The crystallizer is made of very pure copper alloy. The walls of the crystallizer cooled by water dissipate the heat from the solidifying steel. The inner working surface of copper plates contains chromium or nickel to achieve adequate surface hardness. The definition of the heat transfer between the steel blank and the crystallizer, as one of the boundary conditions, is complicated and also key problem [2]. The cooling of the steel blank in crystallizer is a combination of heat transfer by convection, conduction and radiation. The largest amount of heat per time unit is dissipate away from the steel blank in the crystallizer and it is from 10 to 30 % of total heat. In most cases, the crystallizer is cooled by water flowing through the milled slots or drilled channels of the plates, or it is constructed as a tubular, so the whole outer surface is washed by water. The heat transfer passes over every single layer as shown the Fig. 1, which forms an overall resistance against the heat transfer [2].

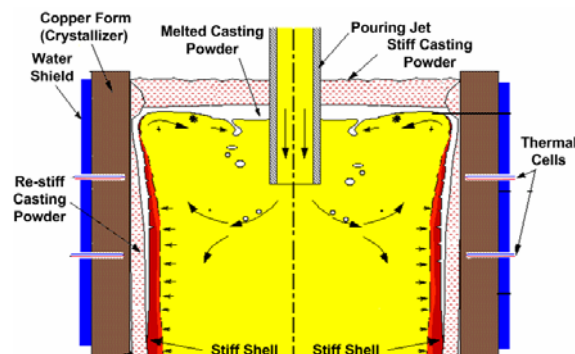


Fig. 1: The crystallizer's operation scheme [2].

## 1.1. The Coefficients of the Heat Transfer in the Crystallizer

The heat flow  $Q_m$  dissipated from the steel blank is given by formula (1) implying that this flow is carried off by cooling water, passing through the crystallizer [3]:

$$\dot{Q}_m = c_w \rho_w F (T_{out} - T_{in}), \quad (1)$$

where  $F$  is the heat flow [ $\text{kg}\cdot\text{s}^{-1}$ ],  $c_w$  is the specific thermal capacity of cooling water [ $\text{J}\cdot\text{kg}^{-1}\cdot\text{K}^{-1}$ ],  $\rho_w$  is the density of cooling water [ $\text{kg}\cdot\text{m}^{-3}$ ],  $T_{out}$  is temperature at the output of the crystallizer [K], and  $T_{in}$  is temperature at the input of the crystallizer [K].

The average heat transfer coefficient on the boundary steel blank – crystallizer can be determined from the equation:

$$htc_m = \frac{\dot{Q}_m}{A(T_{solidus} - T_{out})}, \quad (2)$$

where  $htc_m$  is the heat transfer coefficient of the crystallizer [ $\text{W}\cdot\text{m}^{-2}\cdot\text{K}^{-1}$ ],  $\dot{Q}_m$  is the heat flow of the crystallizer,  $A$  is the area of the crystallizer working surface [ $\text{m}^2$ ],  $T_{solidus}$  is the temperature of the solid phase [K] and  $T_{out}$  is the temperature at the output of the crystallizer [K]. Fig. 2 shows the temperature profile at the steel blank - crystallizer boundary.

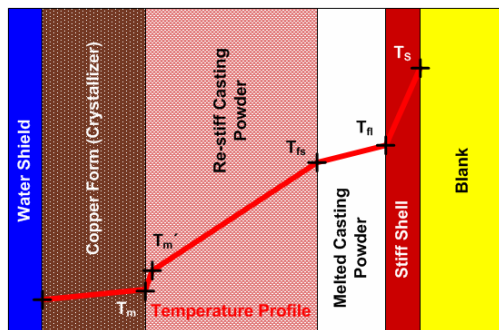


**Fig. 2:** The temperature profile of the steel blank – crystallizer boundary.

From the experimental measurement, in which 44 thermocouples in two lines were installed into the crystallizer, it is possible to observe that the temperature is about values of  $100\text{ }^\circ\text{C}$  at the spot  $T_m$  and do not exceed  $200\text{ }^\circ\text{C}$  [2].

## 2. Optical Fiber DTS Based on the Stimulated Raman Scattering

Optical Fiber DTS (*Distribution Temperature System*) is unique distributed temperature system using optical fiber

as a sensor. Thanks to the advantageous properties of the optical fiber are these sensor systems very interesting and preferable for utilization in the industrial environment [4]. In some actual cases, the optical fiber DTS are nowadays an indispensable tool:

- monitoring of the pipeline leaks,
- monitoring of water leakage in water constructions,
- measurement of temperature profiles of the boreholes into the rock mass (heat pumps).

Optical fiber DTS uses nonlinear phenomena in optical fiber, namely Raman and Brillouin nonlinear scattering. Optical fiber DTS using Brillouin stimulated scattering are able to measure not only the temperature but also mechanical stress along the optical fiber at distances up to 50 km, but due to the higher acquisition costs Raman DTS are currently mostly used in the industrial practises.

### 2.1. The Principle of Operation of Optical Fiber DTS Based on Stimulated Raman Scattering

In the case where we want to determinate the temperature at the certain point  $z$  of the fiber (the distance from the head of the fiber), it is at first important to focus on the characteristic spectrum of the Raman scattering.  $I_S$  represents the intensity of the Stokes part of Raman scattering,  $I_{AS}$  represents the intensity of the anti-Stokes part of Raman scattering. Commonly used lasers in optical fiber DTS based on the stimulated Raman scattering have typical wavelength at 1064 nm [5], [6].

The final mathematical formula describing the principle of operation of optical fiber DTS based on the stimulated Raman scattering is represented by Eq. (3). The final form of the Eq. (3) is a linear combination of the temperature offset (the first part of equation), the difference of the attenuation in the optical fiber (the second part of the equation) and measured temperature based on the ratio of anti-Stokes and Stokes part of the Raman scattering spectrum (the third part of the equation):

$$T(z) \cong T_{REF} \left( 1 + \frac{\Delta\alpha z}{\ln\left(\frac{C_S}{C_{AS}}\right)} + \frac{\ln\left(\frac{I_S(z)}{I_{AS}(z)}\right)}{\ln\left(\frac{C_S}{C_{AS}}\right)} \right), \quad (3)$$

where  $C_S$  and  $C_{AS}$  are constants,  $\Delta\alpha = \alpha_S - \alpha_{AS}$  and is greater than zero,  $T(z)$  is the size of temperature at the spot  $z$  from the head of the optical fiber.

The formula corresponding to the temperature offset  $T_{REF}$  is as follows:

$$T_{REF} = \frac{h\Omega}{k \ln\left(\frac{C_S}{C_{AS}}\right)}, \quad (4)$$

where  $k$  is Boltzmann constant,  $2\pi\Omega$  is red and blue frequency shift and  $h$  is Planck constant.

## 2.2. Optical Meanders in Point Mode

If it is necessary to ensure an accurate localization in the measurement process, it is appropriate to apply optical meanders in the point mode. The point mode means that in some specific spot is created sensory ring from optical fiber. In practice, it is often required to have the sensory ring with as small sizes as possible (inner diameter and length of the optical fiber in the ring). It is obvious that the dimensions of the sensory ring will vary with different parameters of optical fibers [7].

Experimental measurement revealed, that for multimode optical fiber with tight secondary protection (outer diameter 900  $\mu\text{m}$ ) is sensory ring critical inner diameter at value of 3,5 cm, as shown in Fig. 3.

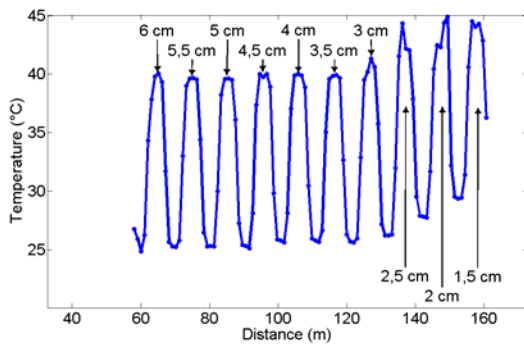


**Fig. 3:** Effect of the inner diameter of the sensory ring on the measured temperature of the water bath (measured together, optical fiber with tight secondary protection, outer diameter 900  $\mu\text{m}$ ).

In the case of using multimode optical fiber with only primary protection (outer diameter 250  $\mu\text{m}$ ), the critical inner diameter of sensory ring decreases to the value of 3 cm, as shown in Fig. 4.

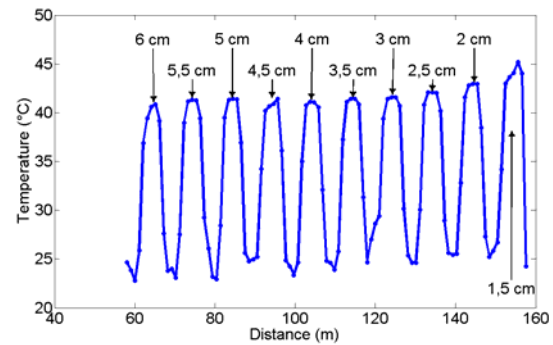


**Fig. 4:** Effect of the inner diameter of the sensory ring on the measured temperature of the water bath (measured together, optical fiber with primary protection, outer diameter 250  $\mu\text{m}$ ).

According to another experimental measurement the length of multimode optical fiber in the single sensory ring has a critical minimal value about 3 m.

## 3. Experimental Utilization of Sensory Rings During High Temperature Measurement

As was found from the experimental measurement of the continual casting in operation using thermocouples, the temperature of crystallizer does not exceed 200  $^{\circ}\text{C}$  and varied around the value of 100  $^{\circ}\text{C}$  [2]. Experimental measurement of the sensory ring parameters made out of multimode optical fiber was carried out in the water bath Memmert at the temperature of 40  $^{\circ}\text{C}$  only. Therefore, it was necessary to verify this method of temperature measurement using sensory ring in measurement of high temperatures.

To verify the applicability of this method for high temperatures measurement was created the configuration consisting of 3 sensory rings. The parameters of the used sensory rings corresponded to the results of the experimental measurements respectively, the inner diameter of the rings was equal to 5 cm, and the length of optical fiber in the ring was 5 m. The distance between individual sensory rings was also 5 m. This configuration allows to assess whether high temperature does not affect the temperature offset calibration and compensation of the optical fiber attenuation (3), as is shown in Fig. 5.

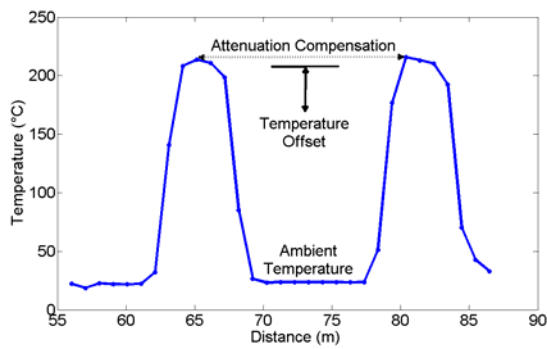


**Fig. 5:** Thermal curves of chosen configuration allowing method analysis in terms of maintaining the temperature offset calibration and compensation of the optical fiber attenuation at high temperatures.

Schematic diagram of the experimental measurement using optical fiber DTS based on the stimulated Raman scattering and configuration of sensory rings shows Fig. 6. The first and the last sensory ring were placed on the ceramic plate inside of the high temperature furnace (ring n.1 and n.3). The middle sensory ring (ring n.2) was placed outside of the high temperature furnace. Target temperature of high temperature furnace was set at 900 °C.

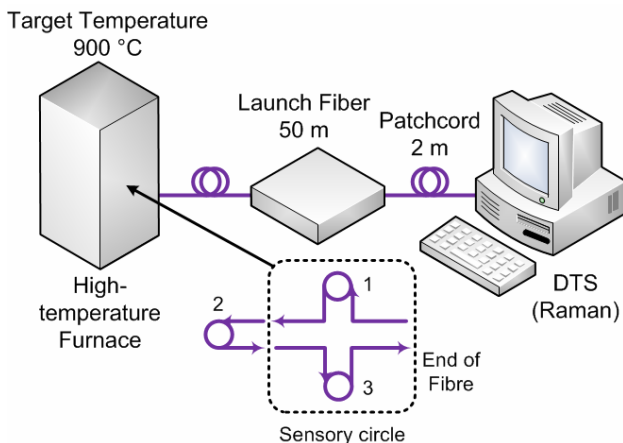


**Fig. 6:** Schematic diagram of the experimental measurement using optical fiber DTS based on the stimulated Raman scattering and configuration of sensory rings.

### 3.1. Sensory Ring from Multimode Optical Fiber with Tight Secondary Protection (Outer Diameter 900 μm)

The sensory rings created from multimode optical fiber with a tight secondary protection were chosen for the initial validation of the method. Ring n.1 was placed near the entrance door of the high temperature furnace, ring n.2 was placed outside of the furnace and ring n.3 was placed in the rear section of the furnace, as shown in Fig. 7.



**Fig. 7:** Placement of sensory rings inside the high temperature furnace. Photo was taken after 45 minutes from the beginning of the process.

The result of the first 30 minutes of the measurement with sensory rings placed in the high temperature furnace shows Fig. 8. The result shows that the disposition inside the furnace was selected incorrectly. The input multimode optical fiber was led to the high temperature furnace through the grommet placed in the upper part of furnace (Fig. 7). The input fiber passes near the heating coil, which caused the tip in measured temperature curves at a distance of 64 m (Fig. 8). Another problem was the temperature distribution inside the furnace. From the measured data, it is obvious that the temperature in the rear section of the furnace is much higher than the temperature near the front door of the furnace.

According to the method displayed in Fig. 5 it is not possible to correctly evaluate method of sensory ring (optical meanders in point mode) in this configuration.

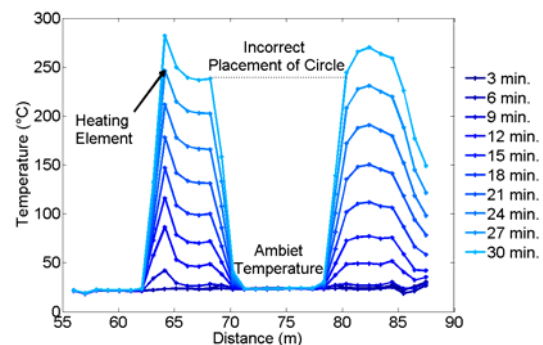


**Fig. 8:** Sensory rings from multimode optical fiber with tight secondary protection placed in high temperature furnace for the time from 0 to 30 minutes. Target temperature 900 °C.

The problem of sensory ring from multimode optical fiber with a tight secondary protection occurs at the temperature of 400 °C. As shown in Fig. 9, the secondary protection (PVC) began to burn, and ring n.1 changed its shape (Fig. 10). These problems significantly affected the measurement of higher temperatures (but only in case of damaged ring).

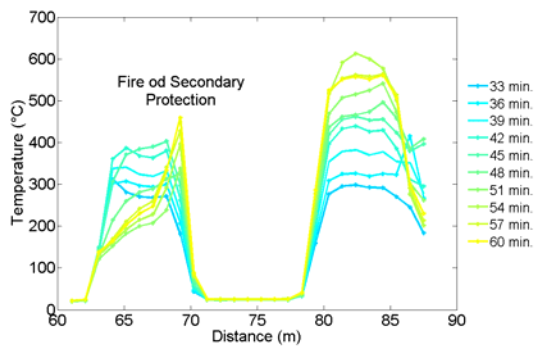


**Fig. 9:** Sensory rings from multimode optical fiber with tight secondary protection placed in high temperature furnace for the time from 33 to 60 minutes. Target temperature 900 °C.



**Fig. 10:** Shape failure of the sensory ring n.1 from multimode optical fiber with tight secondary protection at a temperature higher than 400 °C.

According to these experiments can be said that sensory rings from multimode optical fiber with tight secondary protection are limited in use by the material of secondary protection itself. The flash point of PVC is in the range from 385 to 530 °C, which is the reason, why PVC is not appropriate material for measurement at such high temperatures [8].

### 3.2. Sensory Ring from Multimode Optical Fiber with Primary Protection (Outer Diameter 250 $\mu\text{m}$ )

The configuration with sensory ring from multimode optical fiber with just primary protection was used for the second experimental measurement inside the high temperature furnace. After previous experience, the fiber was guided through the entrance door of the high temperature furnace and sensory rings n.1 and n.3 were placed at each other (Fig. 11).



**Fig. 11:** Detail of disposition of sensory rings n.1 and n.3 inside the high temperature furnace. The photo was taken before the start of the process.

The result of the first 30 minutes of the measurement is shown in Fig. 12.

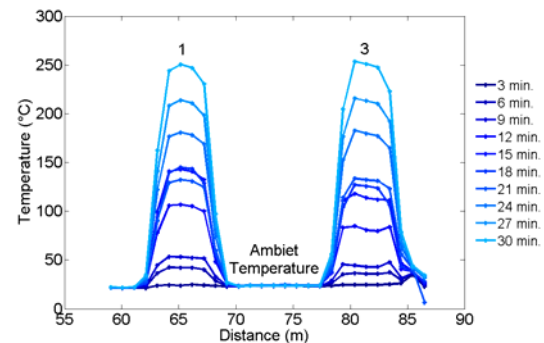


**Fig. 12:** Sensory rings from multimode fiber with primary protection only placed in high temperature furnace for the time from 0 to 30 minutes (target temperature 900 °C).

According to Fig. 12 it is obvious that rings n.1 and n.3 showed different temperatures (for the time from 0 to 21 minutes). We assumed that the lower ring n.3 was cooled by a ceramic plate. Therefore, in the 7<sup>th</sup> iteration of the measurement (21<sup>st</sup> minute) the door of high temperature furnace was opened and the rings were placed next to each other. Our assumption was confirmed because the rings temperatures were aligned in the following time period (from 24 to 30 minutes.).

When the temperature of 330 °C was reached (13<sup>th</sup> iteration of measurement, 39<sup>th</sup> minute.) the temperature in the ring n.3 increased and the temperature in the ring n.1 remained the same. The process was accompanied by a distinctive odour. It was suspected that the draw bands burned out. Therefore, the entranced door of the high temperature furnace was opened between 45<sup>th</sup> and 48<sup>th</sup> minute to check the state of sensory rings. Draw bands burn out confirms Fig. 13.



**Fig. 13:** Burned draw bands used to maintain the shape of sensory rings.

After burn out of the draw band, both rings showed the same temperature. In 19<sup>th</sup> iteration (57<sup>th</sup> minute) at the temperature of 450 °C inside was the entrance door opened again to check the state of the sensory rings. This effect can be observed in Fig. 14 due to decreasing of the temperature from 450 °C to value about 400 °C.

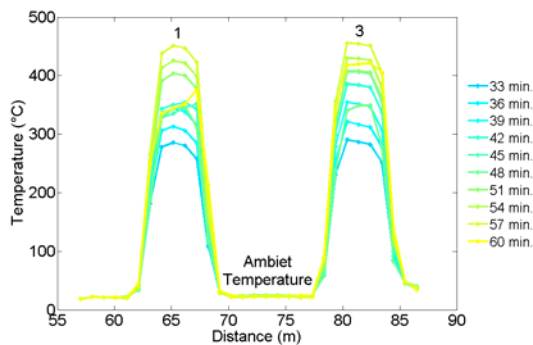


**Fig. 14:** Sensory rings from multimode fiber with primary protection placed in high temperature furnace for the time from 33 to 60 minutes (target temperature 900 °C).

After this check, the door of the furnace was not opened till the end of this measurement. The objective of this measurement was to find out the maximum possible temperature value at which is this method still able to measure correctly, see Fig. 15.

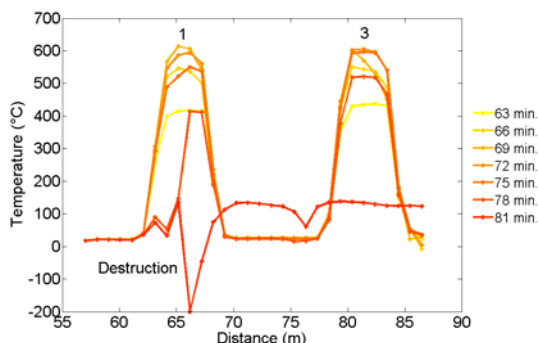


**Fig. 15:** Sensory rings from multimode fiber with primary protection placed in high temperature furnace for the time from 63 to 81 minutes (target temperature 900 °C).

From the Fig. 15, it is clearly visible that the

method is able to measure until the temperature about 600 °C. The destruction of the primary protection layer occurs after exceeding of this temperature. This protection layer held the form of the ring together as a conglutinate (after burn out of the draw band). The collapse of the primary protection layer causes that the multimode optical fiber (core and cladding only) will not keep its original shape. Thanks to its fragility will break apart immediately, when will touch the wall of the furnace (see the 81<sup>st</sup> minute, Fig. 15).

The conclusion of this method experimental verification in high temperature furnace is that for the ideal configuration of the sensory ring is appropriate to use multimode optical fiber with primary protection. This configuration is able to measure the temperatures up to 600 °C. The other advantage of this configuration is that the sensory ring made of multimode optical fiber with just primary protection has a smaller dimension. However in the case of measurement of crystallizer thermal profile, when temperatures are not expected higher than 200 °C, it is possible to use a sensory ring made of multimode optical fiber with a tight secondary protection.

#### 4. Implementation of Sensory Rings on the Crystallizer

For solving of the problems connected with the placement of the sensory rings on the outer shell of the crystallizer was created its model, which has the same outer dimension (in cross section), see Fig. 16.

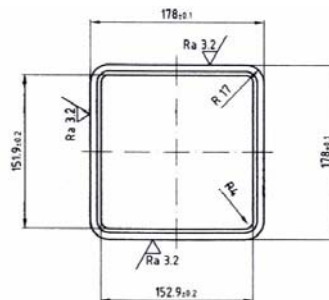


**Fig. 16:** Outer dimensions of the real crystallizer in cross section.

During the construction of this model was for easier fabrication chosen the plate with thickness of 4 mm only. The length of the crystallizer model was set to 600 mm.

The two variants of the sensory rings configurations were chosen for solving of the placement task. It is as a reaction on the question, how to design the configuration of the sensory rings properly, so that the final evaluation will be as simple as possible.

#### 4.1. Option A: Configuration and Calibration

This option includes 4 sensory rings for placement on all 4 sides of the crystallizer in the same level. For reasons of easier manipulation, the sensory rings were produced from the multimode optical fiber with a tight secondary protection (outer diameter 900  $\mu\text{m}$ ), the inner diameter of the ring was 4 cm and the length of the optical fiber in the ring was 4 m. The length of the fiber between adjoining rings was only necessarily long for their connection. The configuration created in this manner was calibrated in the water bath Memmert at the temperature of 40  $^{\circ}\text{C}$ , Fig. 17.

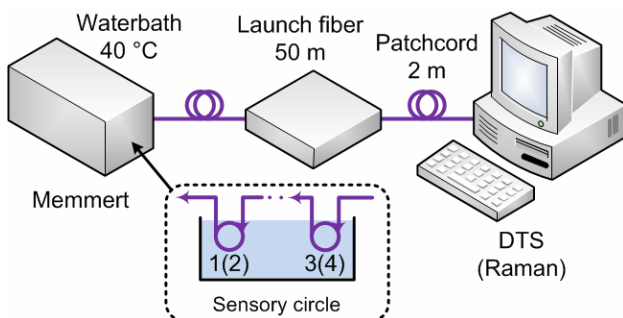


Fig. 17: The calibration of the sensory rings in option A in the water bath Memmert. The temperature of the water bath was 40  $^{\circ}\text{C}$ .

For reasons of too short distance in between the rings the calibration was performed at first with the omission of the sensory rings n.1 and n.3. Then for verifying of the correctness of the settings was the calibration performed with the omission of the sensory rings n.2 and n.4. The results of the calibration are shown in Fig. 18. The deviations were balanced by temperature offset  $T_{ref}$ .

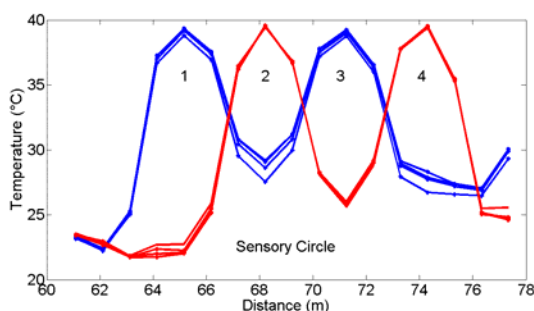


Fig. 18: The results of the calibration and its verification for the configuration of sensory rings in option A.

#### 4.2. Option B: Configuration and Calibration

This option also includes 4 sensory rings for placement on all 4 sides of the crystallizer in the same level. For reasons of easier handling were sensory rings created also from of the multimode optical fiber with tight secondary

protection (outer diameter 900  $\mu\text{m}$ ), the inner ring diameter was 4 cm, as in the previous case, and the length of the optical fiber 4 m also remains the same as in option A.

For better evaluating was decided to set the length of the optical fiber between adjoining sensory rings on 4 m in case of this option. This configuration enables to perform the calibration in the water bath Memmert at once (the temperature of water was set again at the level of 40  $^{\circ}\text{C}$ ). The calibration result is shown in Fig. 19.

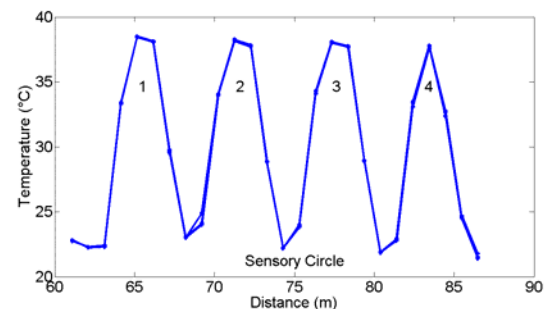


Fig. 19: The results of the calibration for the configuration of sensory rings in option B.

The calibration result presented in Fig. 19 shown that the measured temperature values were about 38  $^{\circ}\text{C}$ . This deviation was balanced by temperature offset  $T_{ref}$  as well.

#### 4.3. Experimental Verification of the Implementation of Sensory Rings on the Crystallizer Model

For experimental verification were both configuration options of the sensory rings placed on the model of the crystallizer by special epoxy adhesive fashioned for high temperatures (Loctite 9492, operating temperature from -55  $^{\circ}\text{C}$  to 180  $^{\circ}\text{C}$ ). The location of sensory rings on the crystallizer was chosen so that on each side of the crystallizer were placed both configuration options of sensory rings at one level (Fig. 20).

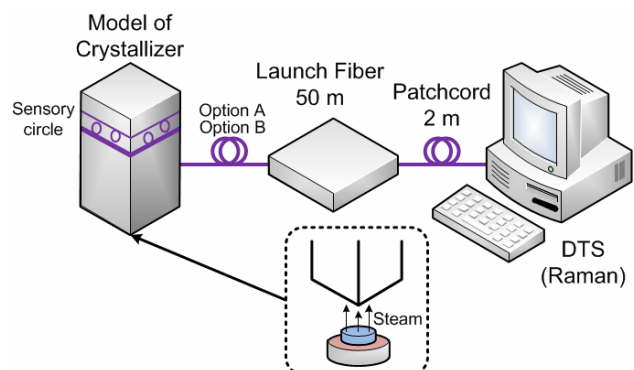


Fig. 20: Experimental verification of the implementation of the sensory rings on the crystallizer model.

At the bottom part of the crystallizer model was

placed a kettle with water that was heated by hot plate. In order to ensure a measurable increasing of temperature on the surface of the crystallizer model was the upper part of the model covered with a metal plate. For reasons of temperature control was under the metal plate placed a sensor of a digital thermometer NTC (Testo 720), see in Fig. 21.



**Fig. 21:** The crystallizer model with covered upper part and NTC sensor of digital thermometer TESTO 720.

The measurement results are shown in Fig. 22 (option A) and in Fig. 23 (option B). The initial conditions are different in ambient temperature, which increased for about 2 °C in case of the first measurement of option B.

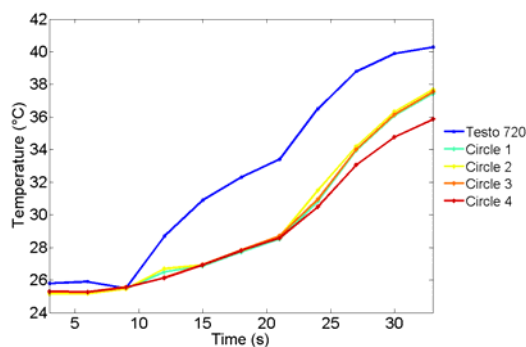


**Fig. 22:** Option A.

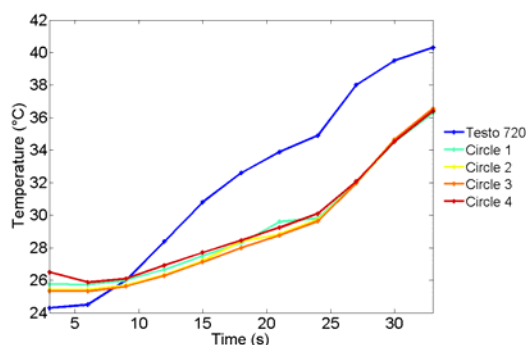


**Fig. 23:** Option B.

## 5. Conclusion

Experimental measurements presented in this article were supposed to verify the applicability of optical meanders in the spot mode (sensory rings) for measurement of the crystallizer temperature profile. The results showed that the best configuration with improved measurement precision was the configuration with two sensory rings at the same level on all 4 sides of the crystallizer. The fibers between two adjoining rings should have the length necessarily needed only for their connection. Ideal sensory material is a multimode optical fiber with primary protection. The reasons are in all respects smaller dimensions (inner diameter, height and width of the ring).

For implementation in real conditions are under consideration milled slots into the outer shell of the crystallizer. After embedding of milled slots by the help of high temperature adhesive a continuous surface will arise for better heat dissipation by flowing water. Fig. 2 shows that the temperature in the milled slots should not increase dramatically, so the optical fiber will be out of damage danger there [2].

## Acknowledgements

This article was supported by project GACR (Czech Science Foundation) GAP108/11/1057 - Synthesis, structure and properties of nanocomposites conducting polymer/phyllsilicate. This work was supported also by the Ministry of Education of the Czech Republic within the project no. SP2012/165 of the VSB-Technical University of Ostrava. The research has been partially supported by the Ministry of Education, Youth and Sports of the Czech Republic through grant CZ.1.07/2.3.00/20.0013.

## References

- [1] KAVICKA, Frantisek, Karel STRANSKY, Bohumil SEKANINA, Jana DOBROVSKA and Josef STETINA. Cooling of a massive casting of ductile cast-iron and its numerical optimization. In: *American Society of Mechanical Engineers, Pressure Vessels and Piping Division (Publication) PVP*. 2010, vol. 4, pp. 617-625. ISBN 978-079184367-3.
- [2] STETINA, Josef. *Dynamicky model teplotniho pole plynule odlevane bramy*. Brno, 2007. Available at: <http://ottp.fme.vutbr.cz/users/stetina/disertace/index.htm>. Dissertation. VUT Brno. Supervisor Frantisek Kavicka.
- [3] DELHALLE, A., Michel LARRECQ, Jacques PETEGNIEF and Jean Paul RADOT. Control of the first shell formation during continuous casting of steel. *Revue de Metallurgie. Cahiers D'Informations Techniques*. 1989, vol. 86, iss. 6, pp. 483-489. ISSN 0035-1563.



- [4] KOUDELKA, P., B. PETRUJOVA, J. LATAL, F. HANACEK, P. SISKA, J. SKAPA and V. VASINEK. Optical fiber distributed sensing system applied in cement concrete commixture research. *Radioengineering*. 2010, vol. 19, no. 1, pp. 172-177. ISSN 1210-2512.
- [5] RODERS, Alan. Distributed optical-fibre sensing. *Measurement Science and Technology* [online]. 1999, vol. 10, no. 8. ISSN 1361-6501. DOI: 10.1088/0957-0233/10/8/201.
- [6] SKAPA, J., J. LATAL, M. PENHAKER, P. KOUDELKA, F. HANACEK and V. VASINEK. Optical fiber distributed temperature sensor in cardiological surgeries. In: *Proceedings of SPIE - The International Society for Optical Engineering*. 2010, vol. 7726, art. no. 77261V. ISBN 978-081948199-3. DOI: 10.1117/12.854309.
- [7] JINGWEI, Ji and Cheng YUAN PING. Temperature ignition criterion of PVC conveyor belts and its application. *Journal of Combustion Science and Technology*. 2006, vol. 12, no. 5, pp. 438-441. ISSN 1006-8740.

## About Authors

**Petr KOUDELKA** was born in 1984 in Prostějov, Czech Republic. In 2006 received Bachelor's degree on VSB-Technical University of Ostrava, Faculty of Electrical Engineering and Computer Science, Department of telecommunications. Two years later he received on the same workplace his Master's degree in the field of Optoelectronics. He is currently Ph.D. student, and he works in the field of wireless optical communications and fiber optic distributed systems.

**Andrej LINER** was born in 1987 in Zlata Moravce. In 2009 received Bachelor's degree on University of Zilina, Faculty of Electrical Engineering, Department of Telecommunications and Multimedia. Two years later he received on the same workplace his Master's degree in the field of Telecommunications and Radio Communications Engineering. He is currently Ph.D. student, and he works in the field of wireless optical communications and fiber optic distributed systems.

**Martin PAPES** was born in 1987 in Nove Zamky. In 2009 received Bachelor's degree on University of Zilina, Faculty of Electrical Engineering, Department of Telecommunications and Multimedia. Two years later he received on the same workplace his Master's degree in

the field of Telecommunications and Radio Communications Engineering. He is currently Ph.D. student, and he works in the field of wireless optical communications and fiber optic distributed systems.

**Jan LATAL** was born in Prostějov. He received his B.Sc. Degree from the VSB-Technical University of Ostrava, Faculty of Electrical Engineering and Computer Science, Dept. of Electronic and Telecommunications in 2006. He received his M.Sc. Degree from the Technical University of Ostrava, Faculty of Electrical Engineering and Computer Science, Dept. of Telecommunications in 2008. Currently in doctor degree studies, he focuses on optical technologies (xPON) and especially on free space optics and Distributed Temperature Sensing systems etc. He is a member of SPIE and IEEE.

**Vladimir VASINEK** was born in Ostrava. In 1980 - he graduated at the Science Faculty of the Palacky University, branch - Physics with specialization in Optoelectronics, RNDr. he obtained at the Science Faculty of the Palacky University at branch Applied Electronics, scientific degree Ph.D. he obtained in the year 1989 at branch Quantum Electronics and Optics, he became an associate professor in 1994 at branch Applied Physics, he is a professor of Electronics and Communication Science since 2007 and he works at this branch at the Department of Telecommunications of the Faculty of Electrical Engineering and Computer Science. His research work is dedicated to optical communications, optical fibers, optoelectronics, optical measurements, optical networks projecting, fiber optic sensors, MW access networks. He is a member of many societies - OSA, SPIE, EOS, Czech Photonics Society, he is a chairman of Ph.D. board at the VSB-Technical University of Ostrava, and he was a member of many boards for habilitation and professor appointment.

**Petr SISKA** was born in 1979 in Kromeriz. In 2005 he finished M.Sc study at VSB-Technical University of Ostrava, Faculty of Electrical Engineering and Computer Science, Dept. of Electronic and Telecommunications. Three years later, he finished Ph.D study in Telecommunication technologies. Currently he is employee of Department of Telecommunications. He is interested in Optical communications, Fiber optic sensors and Distributed Temperature Sensing systems.